

# A simplified approach for stability analysis of slopes reinforced with one row of embedded stabilizing piles

Shiguo Xiao<sup>1,2,3</sup>

Received: 12 April 2016 / Accepted: 6 September 2016 / Published online: 16 September 2016  
© Springer-Verlag Berlin Heidelberg 2016

**Abstract** Embedded stabilizing piles are new anti-slide structures that are unlike traditional stabilizing piles. The pile heads are embedded at a certain depth below the surface of a slope. The piles do not need to support the thrust of the entire upslope sliding mass, and it is, therefore, possible to reduce the sliding thrust on the piles. The embedded depth of the pile heads is an important parameter to maximize the anti-sliding function. Based on an analysis of the stability mechanism of a reinforced landslide with one row of embedded stabilizing piles, a calculation method for the embedded depth of a pile head using limit equilibrium theory is proposed. The related calculation formula is derived in detail using the transfer coefficient method. The proposed method features a close correlation between the embedded depth of a pile head and the design factor of safety of a slope to be reinforced. Additionally, the method can quantitatively demonstrate the relationship that the factor of safety of the slope for the failure mode of the surpassing pile head decreases as the embedded depth of the pile head increases. For a given factor of safety, the range of the maximum bending moment, the maximum shear force on a pile and the lateral displacement at the pile head also can be approximately predicted. Several

calculation examples that are closely related to practical engineering applications are examined to show the convenience and rationality of the proposed method. In addition, the theoretical analysis is compared with the results of the numerical simulation of an actual accumulation landslide control engineering project. The results further demonstrate that the proposed theoretical analysis method is reasonable and applicable.

**Keywords** Embedded stabilizing piles · Embedded depth of pile head · Factor of safety · Limit equilibrium theory

## List of symbols

$c$	Cohesion of the sliding mass
$c_0$	Cohesion of the interface between sliding mass and pile
$c_i$	Cohesion of the $i$ th slip surface upslope of plane AB
$E_i$	Thrust of the $i$ th sliding mass slice on the next one upslope of plane AB
$E_n$	Engineered thrust of the upslope sliding mass of the pile on plane AB
$E_{ph}$	Result of the ultimate resistance on front part ABD of the upslope sliding mass of the pile
$E_{phmin}$	The horizontal component of $E_{ph}$
$F$	Thrust force on the model boundary in the test conducted by Guo and Qin
$F_0$	Resistance against sliding along the interface between the pile and the upslope slide mass
$F_1$	Resistance against sliding along plane AM in Fig. 2c
$F_2$	Resistance against sliding along plane MG in Fig. 2d
$F_s$	Factor of safety of a slope reinforced with piles

✉ Shiguo Xiao  
xiaoshiguo@swjtu.cn

<sup>1</sup> State-province Joint Engineering Laboratory of Spatial Information Technology of High-Speed Rail Safety, Chengdu 610031, China

<sup>2</sup> Key Laboratory of High-speed Railway Engineering, Ministry of Education, Southwest Jiaotong University, Chengdu 610031, China

<sup>3</sup> School of Civil, Mining and Environmental Engineering, University of Wollongong, Wollongong NSW 2522, Australia

$h$	Depth of the sliding mass at the location of the pile	$\phi_e$	Equivalent angle of the internal friction of the localized soil above the original slip surface at the upper area of the pile row
$h_0$	Length of the part of the pile in the slide layer	$\phi_i$	Angle of internal friction of the $i$ th slip surface upslope of plane AB
$h_b$	Depth of the critical slip surface on the boundary in the test conducted by Guo and Qin	$\psi_i$	Transfer coefficient of the $i$ th slide mass slice
$i$	Index		
$l_i$	Length of the $i$ th slip surface upslope of plane AB		
$L_1$	Distance between starting point A of the newborn potential sliding surface and the pile head		
$L_2$	Distance between ending point D of the newborn potential sliding surface and the pile head		
$n$	Number of slices of sliding mass ABF		
$N_1$	Normal compressive force on plane AM in Fig. 2c		
$N_2$	Normal compressive force on plane MG in Fig. 2d		
$R$	Ultimate resistance on plane AJ upslope of the pile		
$R_1$	Force on plane JM upslope of the pile		
$s_1$	Length of the linear section of the original potential slide surface nearest the new generated slip surface		
$s_2$	Length of the linear section of the original potential slide surface nearest the upside of the embedded pile		
$T$	The upslope thrust on the part of a pile in a slide layer		
$W$	Weight of front part ABD of the sliding mass upslope of the pile		
$W_i$	Weight of the $i$ th slide mass slice upslope of plane AB		
$W_a$	Weight of mass AJM upslope of the pile		
$W_b$	Weight of mass JMG upslope of the pile		
$z$	Embedded depth of the pile head		
$\alpha_1$	Dip angle of the original slip surface nearest the new generated slip surface		
$\alpha_2$	Dip angle of the original slip surface nearest the upslope side of the embedded pile		
$\alpha$	Intersection angle between line JM and the segment of the original slip surface nearest the upslope side of the embedded pile		
$\beta_i$	Dip angle of the $i$ th slip surface upslope of plane AB		
$\gamma$	Unit weight of the sliding mass		
$\eta$	Intersection angle between $E_p$ and the vertical direction		
$\theta$	Dip angle of the new generated slip surface		
$\xi$	Ratio of the embedded depth of the pile head over the depth of the sliding mass at the location of the pile		
$\phi$	Angle of internal friction of the slide mass		
$\phi_0$	Friction angle of the interface between the slide mass and pile		

## Introduction

One row of stabilizing piles is a commonly applied engineering structure in landslide control or slope reinforcement works (Randolph 1981; Ito et al. 1981; Chow 1996; Lirer 2012; Tang et al. 2014). It passes the sliding thrust on the load-bearing section (the part of the pile above the slip surface) into the stable layer through the anchoring section (the part of the pile below the slip surface). A traditional stabilizing pile generally has a “full length” structure (Poulos 1995; Lee et al. 1995; Hassiotis et al. 1997; Cai and Ugai 2000; Ausilio et al. 2001; Jeong et al. 2003; He et al. 2015), and the pile head extrudes outside the surface of the slope (i.e., with the part of the pile in the slide layer carrying the thrust of the entire sliding mass at its upper area). From the perspective of the rational loading of the pile, if the load-bearing section is appropriately shortened while the pile location is unchanged, the sliding thrust acting on the stabilizing pile is reduced. The reduction, in turn, facilitates the achievement of the rational stress of the pile. Therefore, a stabilizing pile with a pile head embedded at a certain depth underneath a slope surface (hereafter referred to as an embedded stabilizing pile) is more economical and rational than a full-length stabilizing pile. In addition, for embankment broadening engineering, embedded stabilizing piles can be beneficially used, whereby the piles are first installed, and the fill soil is then added.

To maximize the function of the embedded stabilizing pile, the embedded depth of the pile head is the key issue. If the embedded depth is too shallow, the rational stress of the pile cannot be fully achieved; if it is too deep, the sliding failure might surpass the pile head, thereby compromising the safety of the reinforced slope. To address this problem, a laboratory model test was conducted (Xiong 2000), and the strength reduction finite element method was used in previous research (Lei et al. 2006). In those studies, the embedded depth of the pile head of the embedded stabilizing pile was discussed through an analysis of the stability coefficient of the piled slope. Those approaches presented possibilities for the analysis of the embedded depth of the pile head and the identification of the most dangerous sliding surface that potentially exists in the slope. However, due to the lack of a general theoretical analysis, those methods are not convenient for design engineers in practical engineering. It is, therefore,

necessary to identify a simpler analytical method that does not require complex numerical models or computations to determine the embedded depth of a pile head. The present article focuses on seeking a closed form theoretical solution for determining the rational embedded depth of an embedded stabilizing pile and the corresponding design thrust force on the pile. Through this approach, we intend to simplify the calculation processes involved in these types of problems and promote the wider application of the structure, which has notable merits in engineering practice.

### Stability mechanism of slope reinforcement using embedded stabilizing piles

The sliding failure of a slope is the overall forward and downward movement of the sliding surface (or band) and that of the slide mass lying on it. This type of sliding failure depends principally on the displacement of the sliding surface. Therefore, the key to slope reinforcement using stabilizing piles is the control of the deformation of the sliding surface. That is to say, if the deformation of the sliding surface is suitably limited, the displacement of the slide mass that lies on and moves with the sliding surface is restricted to a great extent. Thus, the stabilizing pile does not necessarily need to restrict the deformation of the entire sliding mass at its upper area. Instead, it can focus on inhibiting the deformation of the sliding surface and part of the sliding mass resting on the surface. An embedded stabilizing pile is sufficient for that purpose. To explain further the mechanism of an embedded stabilizing pile in landslide control or slope reinforcement, presentations are provided to compare and analyze the pressure-transfer mechanism of slope reinforced with both full-length and embedded stabilizing piles. For one row of full-length stabilizing piles, Fig. 1a shows that the deformation of the upslope sliding mass of the load-bearing section of the piles is entirely restricted, and the corresponding landslide thrust is completely acting on the piles. Conversely, for the embedded stabilizing piles (see Fig. 1b), only part of the slide mass resting on the sliding surface is supported, and no restriction is imposed on the soil mass lying above the pile head. That is to say, the deformation of the sliding mass at the upper area of the piles is partially restricted, allowing the pressure of the sliding mass above the pile head to be released to a certain degree. Thus, the corresponding sliding thrust is not acting entirely on the piles. Instead, part of the thrust is transferred down the slope via the soil resting above the pile head. As a result, the sliding thrust acting upon the load-bearing section of an embedded stabilizing pile is smaller than that of the full-length stabilizing pile. Apart from effectively restricting the sliding deformation of the slope, the embedded stabilizing pile also has an effective cost due to its shortened length and reduced thrust.

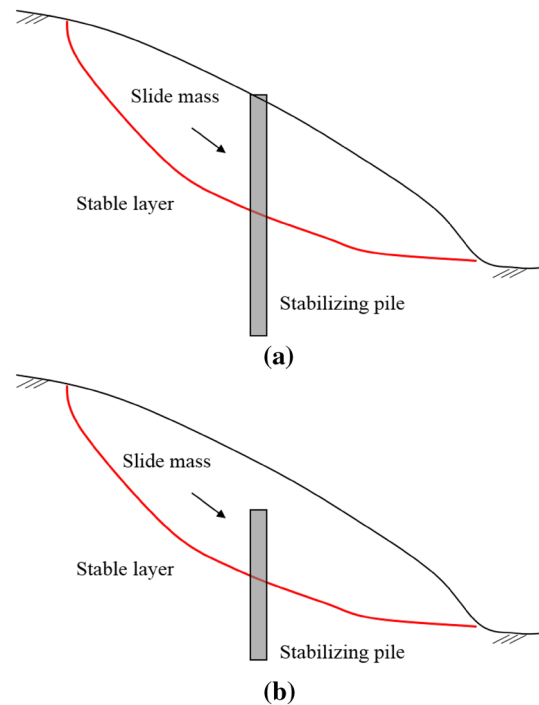
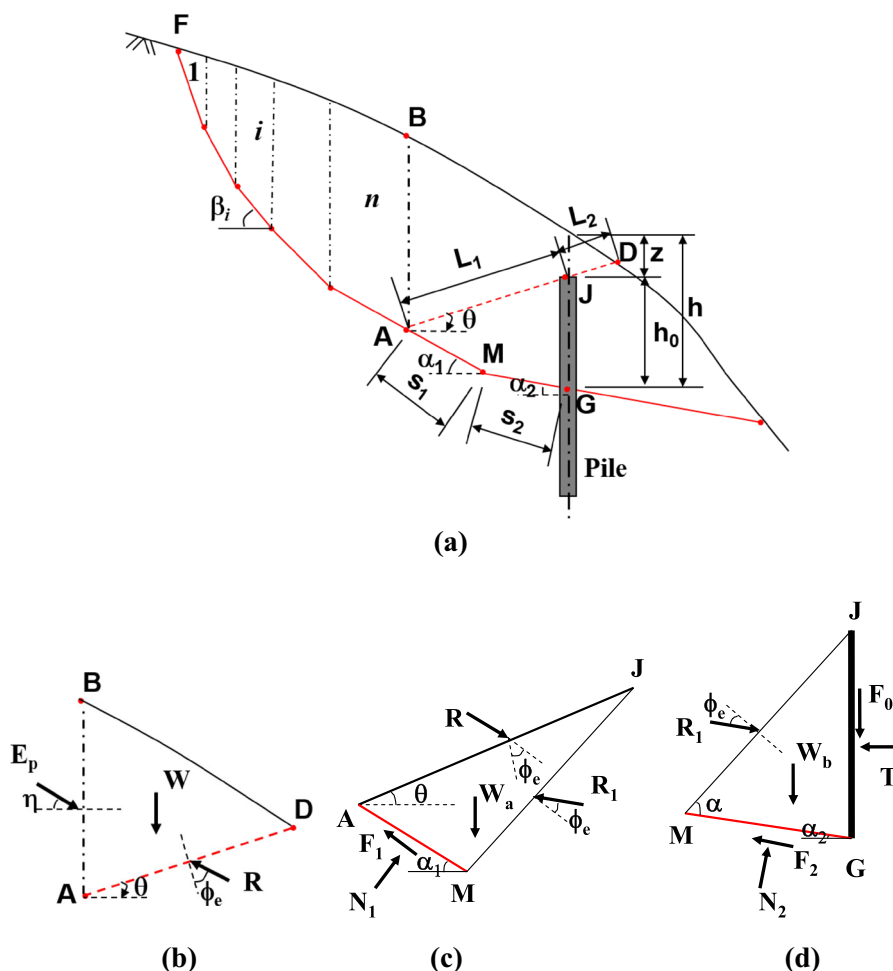


**Fig. 1** Sketch of full-length and embedded stabilizing piles. **a** Full-length type (traditional type), **b** embedded type (new type)

### Analysis model

A graphical analysis of slope reinforcement using embedded stabilizing piles is shown in Fig. 2a, in which the piled slope may slide over the pile head. In the localized sliding mass at the upper area of the pile, a new, but potentially dangerous sliding surface is generated. Compared with the original potential sliding surface of the entire piled slope, the new potential sliding surface is generally shorter. To simplify the analysis, a feature of a curved surface was not considered (i.e., the influence of the cohesive strength on the shape of the sliding surface was disregarded for the soil mass of the localized zone at the upper area of the load-bearing section of the pile), and the new sliding surface was assumed to be a plane. As illustrated in Fig. 2a, if an upwardly auxiliary vertical plane AB is created from intersection A of the new potential sliding surface and the original potential sliding surface, the sliding mass can be divided into a two-part form (i.e., a rear part ABF and a front part ABD). The rear part delivers the sliding thrust directly to the front part, and front part ABD is considered to be under the combined actions of the sliding thrust, self-weight, and the support of the soil mass underneath. Note that the front part is deformed into upward and forward directions under the pressure of the rear part and that the limit thrust it can bear is the ultimate resistance provided that no sliding failure occurs. Therefore, if the ultimate resistance on vertical face AB of front part ABD is greater than the sliding thrust delivered from the rear part ABF, the front part is in a stable state. Otherwise, the

**Fig. 2** Analysis diagrams of a slope reinforced with embedded stabilizing piles. **a** General analysis model, **b** loading mode of mass ABD, **c** loading mode of mass AJM, **d** loading mode of mass MJG



front part loses its stability, and sliding failure occurs. Therefore, for an embedded stabilizing pile with any embedded depth of pile head, the ultimate resistance of the front part of the potential sliding mass at the upper part of the pile can be analyzed first. Subsequently, the validity of the embedded depth can be evaluated in accordance with the magnitude of the sliding thrust delivered from the rear part. Figure 2b–d shows the mechanical analysis model of the sliding masses ABD, AJM, and MJG, respectively.

**Stability analysis method for the piled slope**

**Calculation of the ultimate resistance of the front part ABD of the potential sliding mass at the upper part of the pile**

As illustrated in the graphical analysis in Fig. 2b (for the definitions of each symbol in the figure, refer to the Notation section at the end of the article), for any embedded stabilizing pile with an embedded depth of the pile head  $z$  and for the front part ABD of the potential sliding mass at the upper area

of the pile, the following equation can be obtained according to the limit equilibrium condition:

$$E_p = \frac{\sin(\phi + \theta)}{\sin(\pi/2 + \eta + \phi + \theta)} W, \tag{1}$$

where  $\eta$  varies from 0 to  $\phi$ .

Therefore, the horizontal component of  $E_p$  is

$$E_{ph} = \frac{\sin(\phi + \theta) \cos \eta}{\sin(\pi/2 + \eta + \phi + \theta)} W. \tag{2}$$

According to the extreme principle in mathematics,  $E_{ph}$  can reach a minimum if  $\eta = 0$ . Therefore, the minimum value of  $E_{ph}$  is

$$E_{phmin} = \tan(\phi + \theta) W. \tag{3}$$

**Calculation of the sliding thrust of the rear part ABF of the potential sliding mass at the upper area of the pile**

The upslope sliding thrust on vertical plane AB can be calculated using the transfer coefficient method or

imbalance thrust force method (Bi et al. 2012) to the slide mass ABF divided into  $n$  vertical slices, in which the design factor of safety of the sliding thrust can also be considered. The design sliding thrust  $E_n$  and its corresponding horizontal component  $E_{nh}$  ( $=E_n \times \cos\beta_n$ ) on plane AB are determined in light of Eq. (4) under the condition that  $i$  ranges from 1 to  $n$ :

$$E_i = W_i \sin \beta_i - W_i \cos \beta_i \tan \phi_i / F_s - c_i l_i / F_s + \psi_i E_{i-1}, \tag{4}$$

where  $\psi_i$  can be expressed as:

$$\psi_i = \cos(\beta_{i-1} - \beta_i) - \sin(\beta_{i-1} - \beta_i) \tan \phi_i / F_s. \tag{5}$$

It should be noted that the upslope sliding thrust on vertical plane AB can also be certainly computed using classical Morgenstern-Price method (Morgenstern and Price 1965) or Spencer method (Spencer 1967) with corresponding hypothesis of interslice force function. For the sake of simplicity, the transfer coefficient method mentioned above is just suggested in this paper.

**Comparison of  $E_p$  and  $E_n$**

For any given  $\theta$  equal to the dip angle of line JA ranging from line JF to line JG,  $E_{nh} < E_{phmin}$  demonstrates that the sliding thrust under the design factor of safety is less than the ultimate resistance of the front soil mass, and the embedded depth of the pile head can satisfy the requirement of the design factor of safety and can be optimized. The value of  $z$  can be increased, and additional computations can be carried out in accordance with the above-mentioned calculation method until  $E_{nh} = E_{phmin}$  is achieved. Under such circumstances, the embedded depth of the pile head is theoretically the optimal embedded depth. Conversely,  $E_{nh} > E_{phmin}$  indicates that the embedded depth of the pile head cannot satisfy the requirement of the design factor of safety. The value of  $z$  should then be decreased until  $E_{nh} \leq E_{phmin}$ . Thus, a reasonable embedded depth of the pile head can eventually be determined. Because it is necessary to designate  $\theta$  in advance for any pile head depth  $z$ , the entire calculation process can be carried out via a computer program with finite iterations of the double variables.

**Main calculation procedures**

1. Calculation of factors of safety for the slope with over-pile-top failure modes.  
For different depths of the pile top, namely 0, 0.1  $h$ , 0.2  $h$ , 0.3  $h$ , 0.4  $h$ , 0.5  $h$ , a series of stability coefficients of the slope with over-pile-top failure modes depending on the dip angle of plane AD can be obtained using the above-mentioned method. However, there is a minimum stability coefficient to satisfy the design upslope thrust on the vertical plane AB, which is  $E_{nh} = E_{phmin}$  for any pile top depth. Therefore, the minimum stability coefficient is exactly the factor of safety for the piled slope with the corresponding pile top depth.
2. Judgment of the design failure mode for the slope reinforced with piles.  
Compared with the design factor of safety, if the computed factor of safety is equal to the design factor of safety, the corresponding failure mode is the design failure mode, and the depth of the pile top is the design depth. On the other hand, if the computed factor of safety is greater than the design factor of safety, the surpassing failure mode is not the design failure mode. Therefore, the entire original slip surface upslope of the piles is the design surface for that embedded depth of pile head.
3. Calculation of the upslope thrust on a pile.  
In light of the design failure mode of the surpassing pile head, the upslope thrust on the pile can be determined using limit equilibrium theory. As shown in Fig. 2c and d, provided that the locally original slip surface (including segments AM and MG) on the upslope side of the pile reaches a limit state, the thrust on the pile is:

$$T = \frac{[R_1 \sin(\phi_e + \alpha - \alpha_2) - c s_2 \cos \alpha_2](\cos \alpha_2 + \tan \phi \sin \alpha_2)}{(\cos \alpha_2 + \tan \phi \sin \alpha_2) - \tan \phi_0 (\sin \alpha_2 - \tan \phi \cos \alpha_2)} + \frac{[R_1 \cos(\phi_e + \alpha - \alpha_2) + W_b + c_0 h_0 - c s_2 \sin \alpha_2](\sin \alpha_2 - \tan \phi \cos \alpha_2)}{(\cos \alpha_2 + \tan \phi \sin \alpha_2) - \tan \phi_0 (\sin \alpha_2 - \tan \phi \cos \alpha_2)}, \tag{6}$$

where

$$R_1 = \frac{[R \sin(\phi_e + \theta) - c s_1 \cos \alpha_1](\cos \alpha_1 + \tan \phi \sin \alpha_1)}{(\cos \alpha_1 + \tan \phi \sin \alpha_1) \sin(\phi_e + \alpha - \alpha_2) + (\sin \alpha_1 - \tan \phi \cos \alpha_1) \cos(\phi_e + \alpha - \alpha_2)} + \frac{[R \cos(\phi_e + \theta) + W_a - c s_1 \sin \alpha_1](\sin \alpha_1 - \tan \phi \cos \alpha_1)}{(\cos \alpha_1 + \tan \phi \sin \alpha_1) \sin(\phi_e + \alpha - \alpha_2) + (\sin \alpha_1 - \tan \phi \cos \alpha_1) \cos(\phi_e + \alpha - \alpha_2)},$$

and

$$R = \frac{E_{p\text{hmin}}}{\sin(\phi_e + \theta)} \left[ 1 - \frac{L_2^2}{(L_1 + L_2)^2} \right].$$

If only one segment of the original slip surface remains between the new generated slip surface and the piles (i.e. point M coincides with point A), the thrust on the pile can be expressed as:

$$T = \frac{[R \sin(\phi_e + \theta) - c s_2 \cos \alpha_2](\cos \alpha_2 + \tan \phi \sin \alpha_2)}{(\cos \alpha_2 + \tan \phi \sin \alpha_2) - \tan \phi_0 (\sin \alpha_2 - \tan \phi \cos \alpha_2)} + \frac{[R \cos(\phi_e + \theta) + W_b + c_0 h_0 - c s_2 \sin \alpha_2](\sin \alpha_2 - \tan \phi \cos \alpha_2)}{(\cos \alpha_2 + \tan \phi \sin \alpha_2) - \tan \phi_0 (\sin \alpha_2 - \tan \phi \cos \alpha_2)}. \tag{7}$$

For the failure mode of a non-surpassing pile head, the upslope thrust on the pile can be determined by the transfer coefficient method mentioned above on the basis of the original slip surface at the upper area of piles.

4. Computation of the internal forces of a pile. After the upslope thrust  $T$  on practical stabilizing piles used in large slope or landslide control is determined using Eqs. (6) or (7), the responses, including the bending moment and shear force of a stabilizing pile, can be resolved using a plastic (sliding layer)-elastic-plastic (stable layer) model (Guo 2013). For a piled slope, the upslope thrust on piles can be regarded as the lower bound when surpassing failure happens with the shear strength of the locally original slip surface upslope of the piles being assumed to develop entirely. But the upslope thrust reaches the upper bound under the condition that the critical slip surface of the piled slope remains the original slip surface of the slope without piles. Therefore, the internal forces of piles corresponding to surpassing failure could be viewed as the lower bound. However, the upper bound of the internal forces can be determined based wholly on the original slip surface upslope of the piles.

### Verification examples

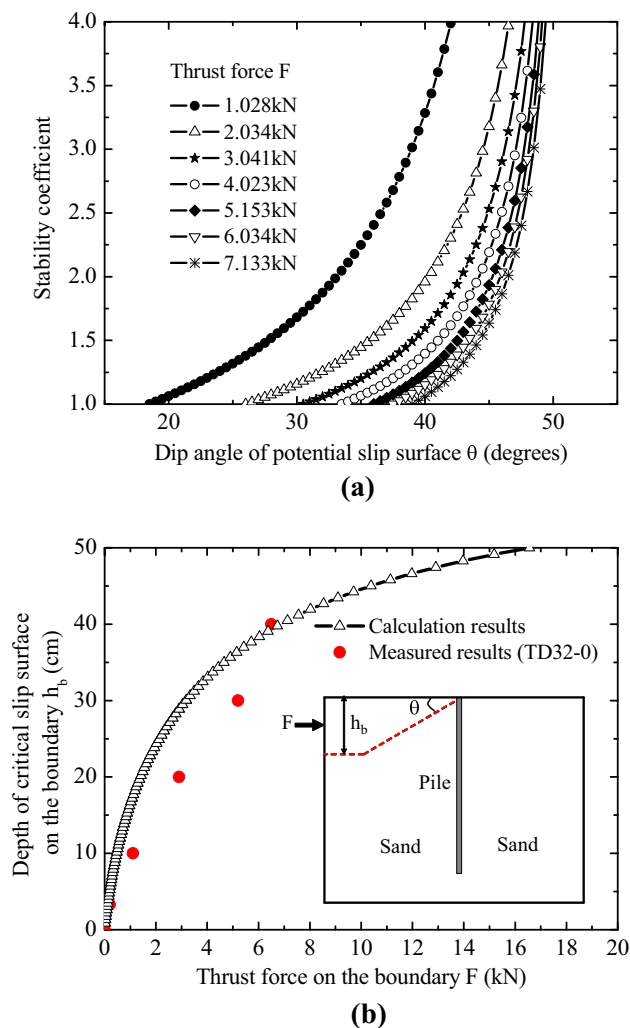
#### A laboratory test example

A laboratory model pile test was conducted to determine pile responses under lateral soil movement (Guo and Qin 2010). Thrust forces were exerted on the model boundary to cause the sand surrounding the pile to move in the test. Using the proposed method, factors of safety were determined under various thrust forces. As shown in Fig. 3a, the

factor of safety for the surrounding sand pile grew as the dip angle of the potential slip surface increased, which indicates that the critical slip mode of the soil is a linear failure mode. The depth of the critical slip surface on the boundary where the thrust forces were applied increased as the thrust force increased (see Fig. 3b). Additionally, Fig. 3b shows that the theoretical results are in good agreement with the measured results, which indicates that the proposed method is reasonable.

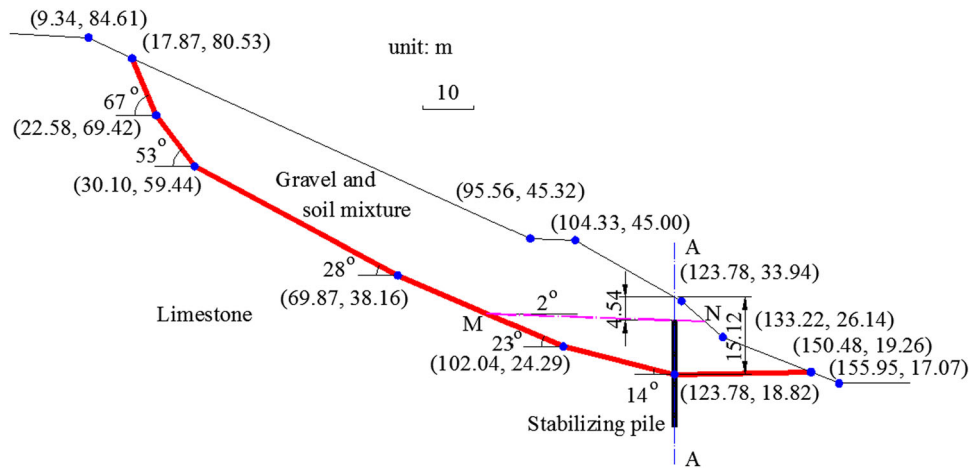
#### An engineering example

Figure 4 shows an accumulation landslide with a potential polyline slip surface (i.e., a bedrock surface) in Sichuan Province, China. The profile of the slope generally consists of two layers, as follows: an upper layer, which is a mixture



**Fig. 3** Analysis results of stability for the test model under various thrust forces on the boundary. **a** Stability coefficient versus dip angle of the potential slip surface, **b** depth of the critical slip surface on the boundary

**Fig. 4** Cross section of the engineered slope example



of gravel and soil and a lower layer, which is stable limestone. The bedrock surface of the slope is the original potential sliding surface of the slope mass. The main properties of the slope are shown in Table 1. Mechanical parameters of the slip surface are equal to those of the gravel and soil mixture. One row of stabilizing piles with a pile spacing of 5 m has been designed for installation at the location of section AA to increase the factor of safety of the slope from a little above 1.0 to the design factor 1.20. The pile arrangement is shown in Fig. 4, and the properties of the piles are also given in Table 1. Cross section of a pile is 2 m × 3 m, and the length of the pile is 21.2 m. The depth of the slide mass at the location of piles is 15.12 m,  $c_0 = 0$ ,  $\phi_0 = 10^\circ$ ,  $\phi_e = 22.9^\circ$ , and the lateral ultimate bearing capacity of the stable layer is 1000 kPa.

The stability coefficients of the slope under the conditions of various depths of pile top or embedded ratios  $\zeta$  are shown in Fig. 5, which indicates that the stability coefficient decreases as the embedded depth of pile head increases for each  $\zeta$  and that there is minimum stability coefficient with  $\theta$  varying that is exactly the factor of safety of the slope with piles. For each  $\zeta$ , the factor of safety obtained using the proposed method is identical to two-dimensional numerical simulation result by **Phase<sup>2</sup>** program (Rocscience Inc. 2014). As shown in Fig. 5, when the depth of pile top reaches 4.54 m ( $\zeta = 0.3$ ), the factor of safety of the slope with piles is 1.230. Hence, a depth of pile top of 0.3  $h$  will just conservatively meet the design requirement. As shown in Fig. 4, the dip angle of the potential new slip surface MN at the upper area of the piles is  $\theta = -2^\circ$  ( $\theta$  is positive clockwise, see Fig. 2). The corresponding maximum

bending moment and shear force of a pile are 30,745.52–48,614.49 kN.m and 5288.56–7988.73 kN, respectively (see Fig. 6). Additionally, as shown in Fig. 6, the theoretical calculation results of the pile responses are in good agreement with the numerical simulation results. Therefore, the results indicate that an embedded depth of the pile head of 4.54 m can be applied in the project.

## Discussion

### Comparison of the theoretical and numerical analysis results

A numerical simulation analysis was adopted to verify the results of the theoretical analysis of the engineering project and demonstrate the rationality of the method. A three-dimensional (3D) finite element model was built based on a rational embedded depth of 4.54 m (0.3  $h$ ) obtained via the theoretical analysis mentioned above. As shown in Fig. 7, the slope model was divided into eight-node hexahedron elements, which produced 87,920 elements in all. An ideal elastoplastic constitutive model and Mohr–Coulomb yield criterion were used for the slope material. A non-associated flow rule was adopted as well. The pile was taken as an elastic body. Using the strength reduction finite element method by **Flac3D** program (Itasca Consulting Group, 2012), we obtained a slope factor of safety of 1.20, which is close to the factor of safety of 1.23 determined using the theoretical calculation. The distribution results of the maximum shear

**Table 1** Main parameters of the slope example

Material type	Unit weight (kN/m <sup>3</sup> )	Cohesion (kPa)	Angle of internal friction (°)	Elastic modulus (MPa)	Poisson's ratio
Gravel and soil mixture	22	14.5	22	50	0.33
Limestone	23	500	38	600	0.25
Stabilizing pile	25	–	–	30,000	0.22

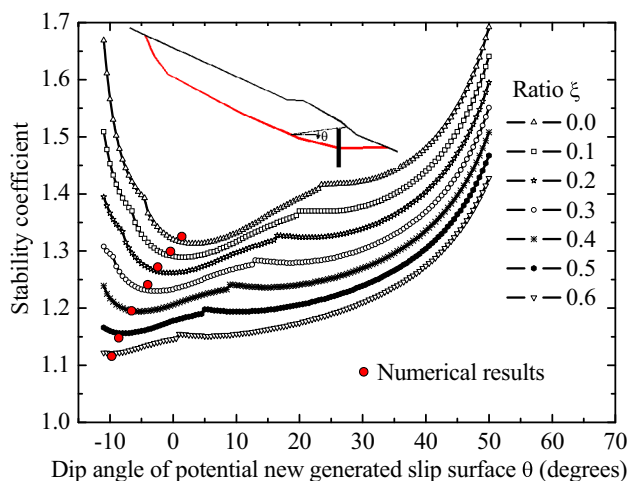


**Fig. 5** Stability coefficients for the failure mode of the surpassing pile head as a function of dip angle  $\theta$  with different ratios  $\xi$

strain increment of the slope under a strength reduction factor of 1.20 are shown in Fig. 8. The potential slide failure mode of the slope is the slide failure surpassing the pile head. As shown in Fig. 9, the theoretical analysis and the numerical simulation results of the most dangerous sliding surface of the slope have been placed on the same diagram. The diagram shows that the most dangerous potential sliding surface obtained using the proposed theoretical calculation was satisfactorily close to that obtained by the numerical analysis. In addition, the factor of safety of the slope determined using the numerical analysis was also very close to that evaluated using the proposed theoretical method. Therefore, the rationality of the proposed theoretical analysis method has been adequately verified.

**Treatment of the sliding mass with cohesion**

In practice, the sliding mass upslope of the pile row is probably a cohesive soil mass. To use the above-mentioned method in that case, it is necessary to determine the equivalent angle of the internal friction of the localized soil mass resting on the original potential sliding surface at the upper area of the pile. This can be approximately achieved by adopting the method that the original slope factor of safety retains the unvaried value in the case of the simplified soil mass without cohesion.

**Influence of the depth of the pile top on the stability of the reinforced slope and responses of the piles**

The depth of the pile top has an important effect on the stability of a slope reinforced with stabilizing piles and the corresponding responses of the piles. As shown in Fig. 10a,

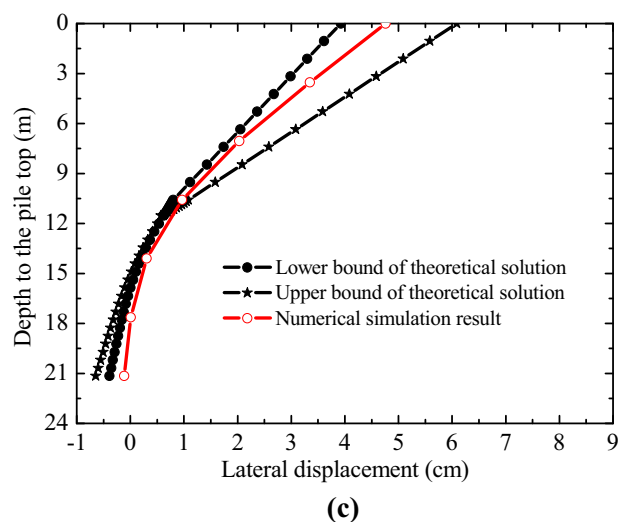
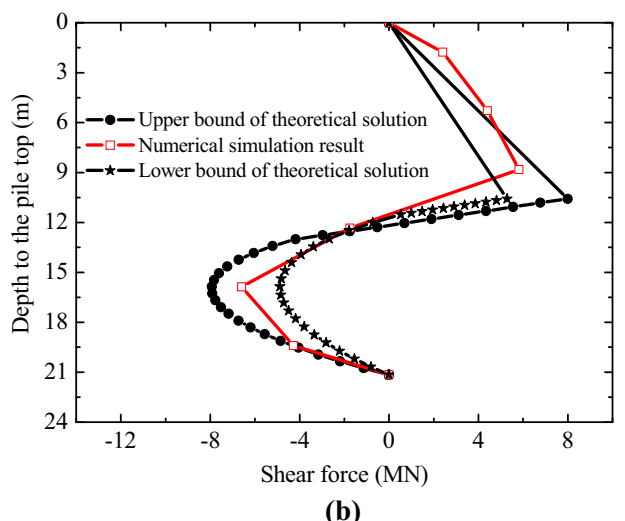
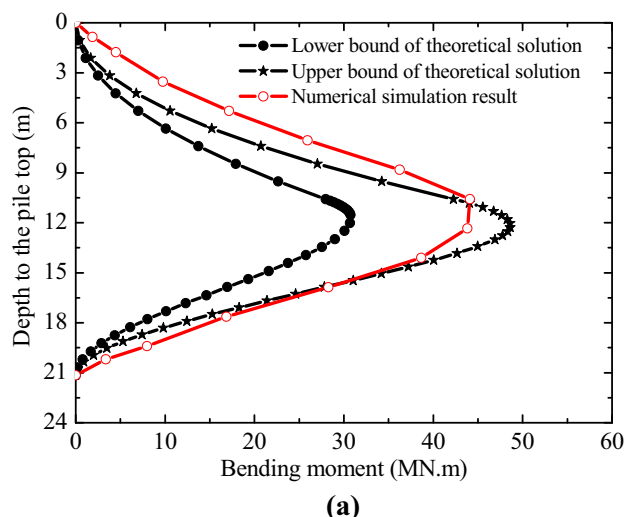


**Fig. 6** Design internal forces of embedded piles in the example. **a** Bending moment, **b** shear force, **c** lateral displacement



**Fig. 7** Numerical simulation model for the reinforced slope example

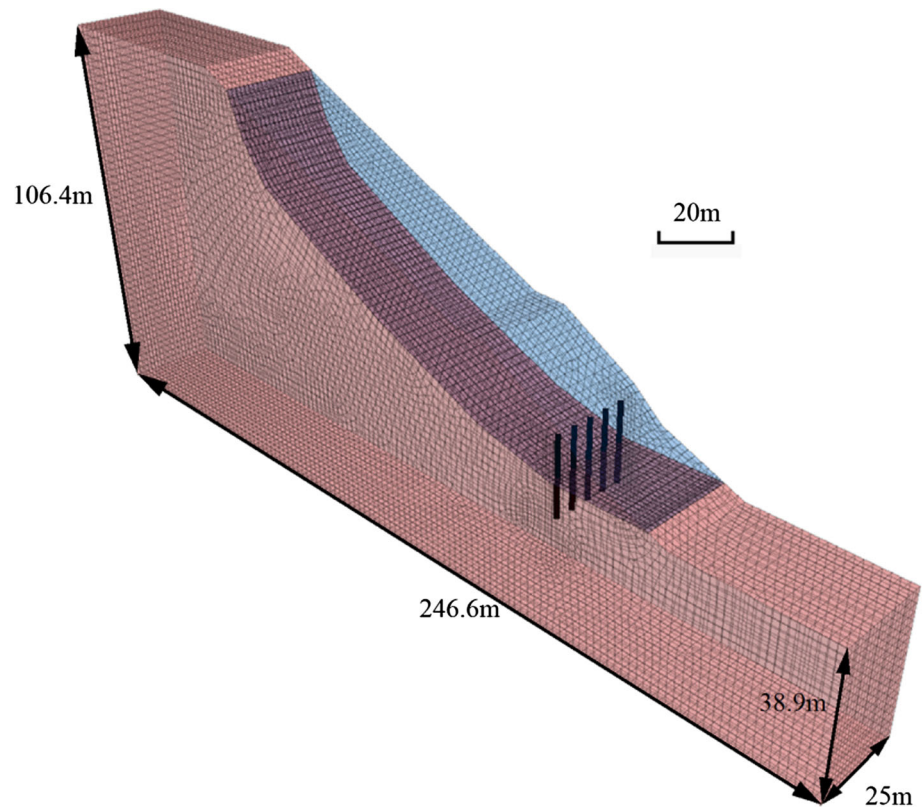
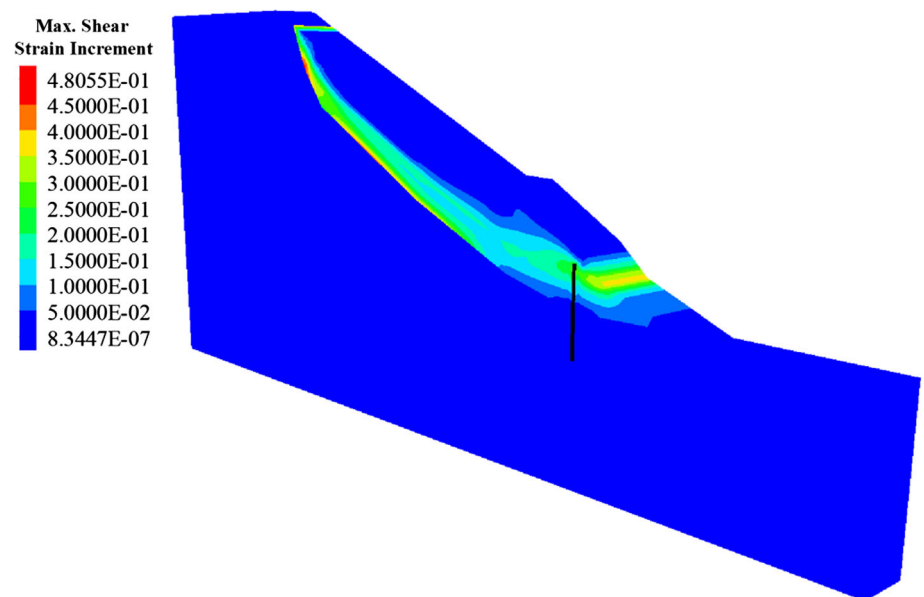


**Fig. 8** Distribution of the maximum shear strain increment in the reinforced slope with a strength reduction factor of 1.20



the factor of safety of the reinforced slope decreases as the depth of the pile top increases. In addition, it further indicates that the results from the present method are in good agreement with the numerical simulation results. In theory, when the ratio of the depth of the pile top over the depth of the slide mass at the location of the pile reaches 0.38, the stability coefficient for the surpassing pile top

failure mode exactly satisfies the design factor of safety. Therefore, the maximum depth of the pile head is 5.74 m ( $=0.38 \times 15.12$  m). If the practical depth of the pile top is more than 5.74 m, the reinforced landslide cannot be stable with a factor of safety of 1.20. For the rigid piles in the slope example, profiles of the bending moment, shear force, and deflection of the pile under various embedded

**Fig. 9** Comparison of the proposed theoretical analysis and the numerical simulation for the potential most dangerous slip surface generated (intermediate profile of the 3D numerical model)

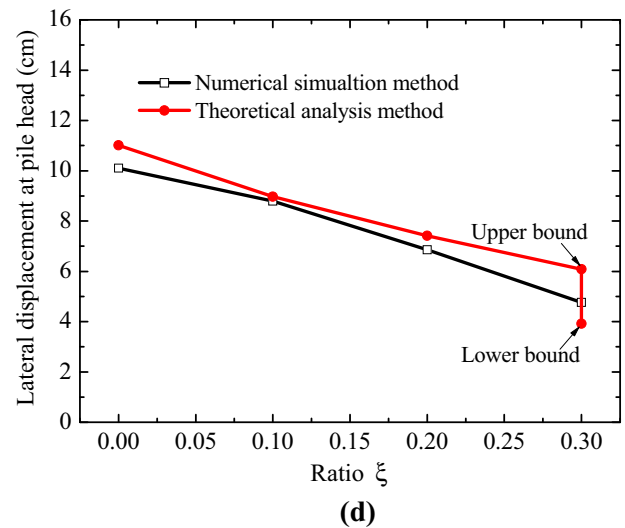
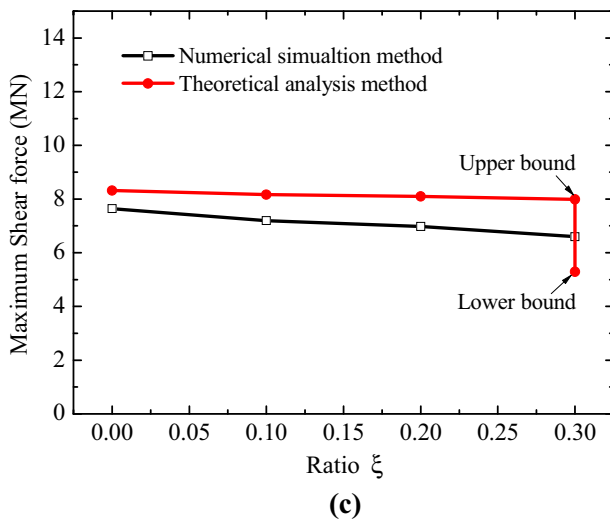
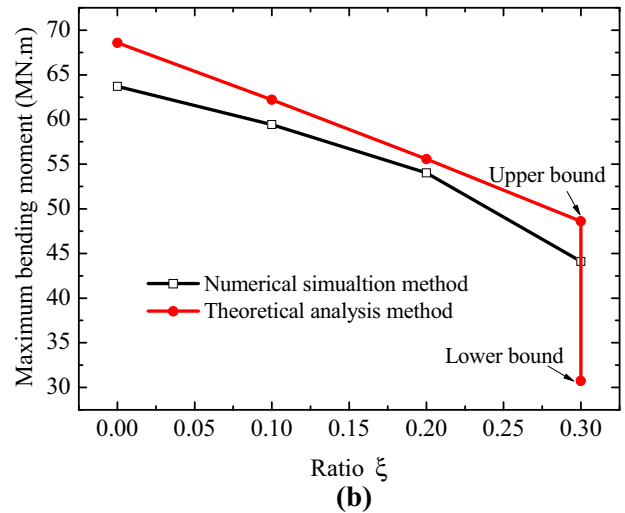
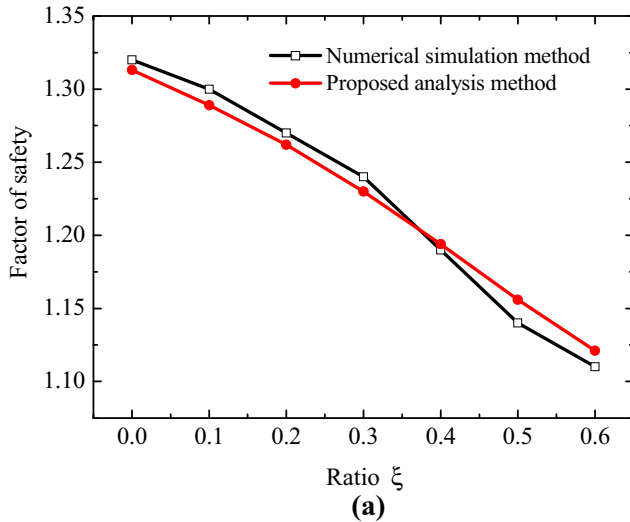
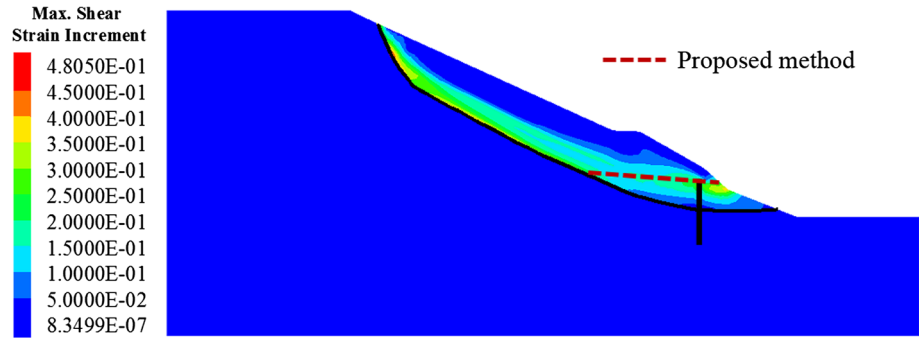


**Fig. 10** Influence of the embedded depth of the pile top on the stability of the reinforced slope and the responses of the piles in the slope example. **a** Factor of safety, **b** maximum bending moment, **c** maximum shear force, **d** lateral displacement at the pile head

depths of the pile top are similar to those shown in Fig. 6, respectively. Therefore, the maximum bending moment, shear force of the pile and the lateral displacement at the pile head influenced by the depth of pile top are just discussed here. In fact, as the depth of the pile top increases

under the condition that it does not exceed 5.74 m, the maximum bending moment, the shear force of the pile and the lateral displacement at the pile head gradually decrease (see Fig. 10b–d, respectively). The responses of the pile determined using the analytical method are slightly greater

than those using the numerical results, which shows that the proposed method is acceptable. Therefore, it can be safely stated that increasing the embedded depth of the pile top to some extent will help reduce the internal forces and the lateral displacement of the pile.

### Matters requiring attention when determining the rational embedded depth of the pile head

In actual engineering practice and from the perspective of the feasibility of practical operation, it is important to focus on the following aspects when determining the rational embedded depth of a pile head using theoretical calculations.

1. To ensure comprehensive, yet technically and economically rational methods and results under various circumstances and in consideration of the results of actual cases in China, we propose that the embedded depth of the pile head not exceed  $0.5 h$  or drop below  $0.2 h$ .
2. Based on a large number of stabilizing pile design examples in China, the length of the embedded stabilizing pile in the stable layer should be equal to or slightly longer than that in the slide layer to ensure the overall stability of the pile.

### Two additional examples

1. A broadening embankment slope  
The embankment shown in Fig. 11 needs to be broadened from point B to point F for the purpose of improving its application function. The design slip surface, which has a cohesion of 5 kPa and an internal

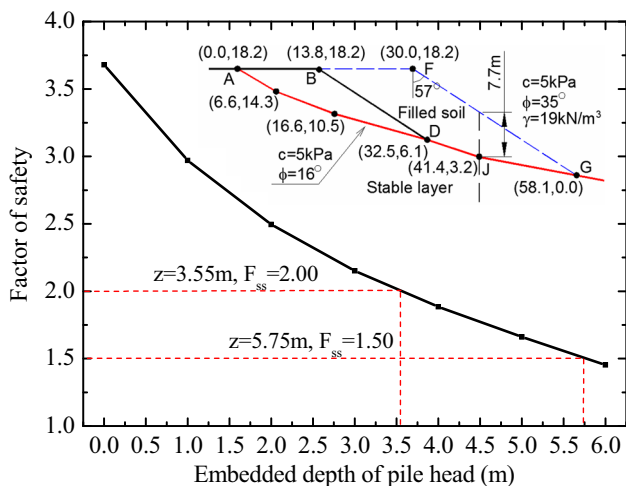


Fig. 11 Relationship between the factor of safety and the embedded depth of the pile head in a broadening embankment slope

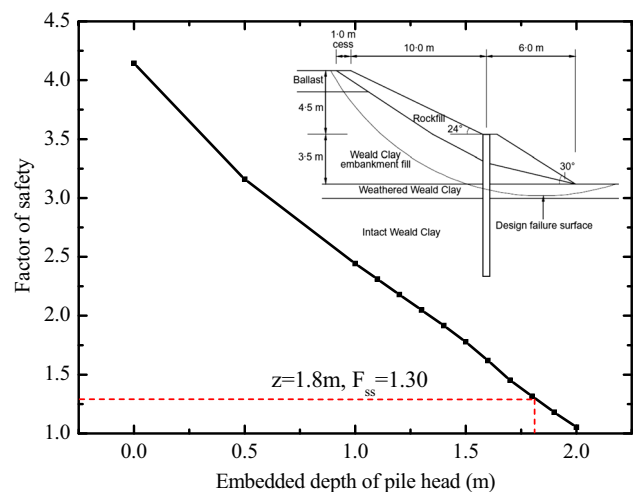


Fig. 12 Relationship between the factor of safety and the embedded depth of the pile head in a filled railway embankment slope

angle of friction of  $16^\circ$ , lies between the upper fill soil and the lower stable layer. The properties of the fill soil are given in Fig. 11, and the dip angle of the extended slope surface FG parallel to the original slope BD is  $57^\circ$ . The factor of safety of the original slope is 1.03, and the extended embankment slope is designed to be sufficiently stable, with a factor of safety of at least 1.50. To increase the stability of the extended embankment slope, one row of piles can be embedded at location J to a depth of 7.7 m before adding the fill soil. The variation in the factor of safety of the extended embankment slope with the embedded depth of the pile head per the proposed method is shown in Fig. 9. The figure shows that the factor of safety reached 1.50 and 2.00 when the embedded depths were 5.75 m and 3.55 m, respectively.

2. A filled railway embankment slope.  
A filled embankment slope in a railway engineering project (Smethurst and Powrie 2007) is shown in Fig. 12. One row of full-length piles was installed to increase the factor of safety of the slope from slightly greater than 1.0 to the specified 1.30. However, the design can be optimized using the present method. As shown in Fig. 12, to maintain the same stability of the slope, the depth of the pile head could be 1.8 m, which would result in shorter piles and greater cost effectiveness.

### Conclusions

The embedded stabilizing piles restricted the partial deformation of the sliding mass and partially resisted the sliding thrust of the entire sliding mass at the upper area of the piles. Compared with full-length piles used for

controlling landslides with the original potential slip surface being a bedrock surface, the embedded type has the advantage of achieving a rational pile stress state. Especially, this type of pile is completely suitable for embankment broadening engineering. A reasonable embedded depth of the pile head is the key to guaranteeing the rational application of the technique and the cost effectiveness of this type of anti-slide structure. Based on the investigation carried out in this study, the following conclusions are drawn.

1. Based on limit equilibrium theory and the transfer coefficient method of the sliding thrust, the rational embedded depth of the pile head of an embedded stabilizing pile can be determined using an approximate theoretical analysis method. Corresponding reasonable embedded depths of pile heads and the thrust forces on piles for a reinforced landslide or slope under different design factors of safety can also be determined. The lower and upper bound values of the internal forces of embedded piles can be determined based on the surpassing failure and original slip mode upslope of the piles, respectively.
2. The embedded depth of the pile head has a significant influence on the stability of a landslide or slope reinforced with one row of stabilizing piles and on the corresponding responses of the piles. The factor of safety for the reinforced slope decreases as the embedded depth of pile top increases; however, the internal forces of the pile also decrease given the same variation of the pile head.
3. The rational embedded depth of the pile head of an embedded stabilizing pile is influenced by a number of factors that include the internal friction angle and the cohesion of the sliding mass and sliding surface, the shape and dip angle of the sliding surface at the upper area of the pile, the thickness of the sliding mass at the location of the pile, and the design factor of safety of the reinforced slope. In engineering design and calculation, attention should be paid to the influence of these important factors on the results of pile design calculations.

**Acknowledgments** This research was supported by the National Natural Science Foundation of China (Grant Nos. 51278430 and 51578466), the Program for New Century Excellent Talents in University (NCET-13-0976), and the National Basic Research Program of China (973 Program) (Grant No. 2010CB732105). The author is also very grateful to Dr. Wei-dong Guo for generously

providing test data and to Prof. Yingren Zheng and Anhong Li for their helpful suggestions.

## References

- Ausilio E, Conte E, Dente G (2001) Stability analysis of slopes reinforced with piles. *Comput Geotech* 28:591–611
- Bi R, Ehret D, Xiang W, Rohn J, Schleier M, Jiang J (2012) Landslide reliability analysis based on transfer coefficient method: a case study from three gorges reservoir. *J Earth Sci* 23(2):187–198
- Cai F, Ugai K (2000) Numerical analysis of the stability of a slope reinforced with piles. *Soils Found* 40(1):73–84
- Chow YK (1996) Analysis of piles used for slope stabilization. *Int J Numer Anal Meth Geomech* 20:635–646
- Guo WD (2013) Pu-based solutions for slope stabilizing piles. *Int J Geomech* 13:292–310
- Guo WD, Qin HY (2010) Thrust and bending moment of rigid piles subjected to moving soil. *Can Geotech J* 47:180–196
- Hassiotis S, Chameau JL, Gunaratne M (1997) Design method for stabilization of slopes with piles. *J Geotech Geo-environ Eng* 123(4):314–322
- He Y, Hazarika H, Yasufuku N, Han Z (2015) Evaluating the effect of slope angle on the distribution of the soil–pile pressure acting on stabilizing piles in sandy slopes. *Comput Geotech* 69:153–165
- Itasca Consulting Group (2012) FLAC3D 5.0 manual. Itasca Consulting Group, Minneapolis
- Ito T, Matsui T, Hong WP (1981) Design method for stabilizing piles against landslide—one row of piles. *Soils Found* 21(1):21–37
- Jeong S, Kim B, Won JN, Lee JH (2003) Uncoupled analysis of stabilizing piles in weathered slopes. *Comput Geotech* 30:671–682
- Lee Y, Hull TS, Poulos HG (1995) Simplified pile-slope stability analysis. *Comput Geotech* 17:1–16
- Lei WJ, Zheng YR, Feng XT (2006) Limit analysis of slope stabilized by deeply embedded piles with finite element method. *Chin J Rock Mech Eng* 25(1):27–33 (in Chinese)
- Lirer S (2012) Landslide stabilizing piles: experimental evidences and numerical interpretation. *Eng Geol* 149–150:70–77
- Morgenstern NR, Price V (1965) The analysis of the stability of general slip surface. *Geotechnique* 15:79–93
- Poulos HG (1995) Design of reinforcing piles to increase slope stability. *Can Geotech J* 32:808–818
- Randolph MF (1981) The response of flexible piles to lateral loading. *Geotechnique* 31(2):247–259
- Rocscience Inc (2014) Shear strength reduction analysis. [https://www.rocscience.com/help/phase2/webhelp/tutorials/Phase2\\_Tutorials.htm](https://www.rocscience.com/help/phase2/webhelp/tutorials/Phase2_Tutorials.htm). Accessed 20 Nov 2014
- Smethurst JA, Powrie W (2007) Monitoring and analysis of the bending behaviour of discrete piles used to stabilise a railway embankment. *Geotechnique* 57(8):663–677
- Spencer E (1967) A method of analysis of embankments assuming parallel inter-slice forces. *Geotechnique* 17:11–26
- Tang H, Hu X, Xu C, Li C, Yong R, Wang L (2014) A novel approach for determining landslide pushing force based on landslide-pile interactions. *Eng Geol* 182:15–24
- Xiong Z (2000) Force distribution rule of deeply embedded anti-slide pile. *China Railway Science* 21(1):48–51 (in Chinese)